Journal of Nanoscience and Technology 2(2) (2016) 100–103

ISSN: 2455-0191

Contents List available at JACS Directory

Journal of Nanoscience and Technology

journal homepage: www.jacsdirectory.com/jnst

Sputtering Synthesis and Thermal Annealing Effect on Gold Nanoparticles in Al_2O_3 Matrix

A. Belahmar, A. Chouiyakh*

Department of Physics, Laboratory of Condensed Matter Physics, IBN Tofail University, B.P.133, 14000, Kenitra, Morocco.

ARTICLE DETAILS

Article history:
Received 16 March 2016
Accepted 27 March 2016
Available online 08 April 2016

Keywords:
Au Nanoparticles
Lattice Parameter
Thermal Expansion

ABSTRACT

Gold-Alumina nano composite thin films were prepared by RF-magnetron sputtering technique on glass substrate at room temperature. Subsequent thermal treatment was used to promote gold nano clusters formation. After annealing, an increase of size accompanied by an increase of the lattice constant parameter is observed. A value of the surface stress coefficient of gold is $f = 3.11$ N/m has been obtained and a value of lattice thermal expansion coefficient of gold $\alpha_{gold}(T) = 2.6 \times 10^{-5}$/ °C is achieved. Broad band absorption with maximum absorbance at around 500 nm characteristic of gold nanoclusters was observed after heat treatment. Experimental optical absorption spectra were modeled by the modified Mie theory. A red sift of the plasmon peak is obtained with increasing the annealing temperature.

1. Introduction

Materials tailored at the nanoscale, e.g. in the form of nanoparticles, have unique physical and chemical properties compared to their bulk form [1]. Among them, noble metals are the most studied plasmonic materials when they are embedded in a dielectric matrix they manifest surface plasmon resonance (SPR) in the visible range [2-4]. SPR is the unique property of noble metal nanoparticles due to its resonant collective oscillation of electrons in the presence of electromagnetic field. The SPR peak position wavelength can be tailored by varying the size, shape, inter particles separation, dielectric constant of metal nanoparticles as well as the embedding matrix which has been investigated by several researchers [5–9]. The ability to integrate metal nanoparticles into biological systems with general lack of toxicity has had greatest impact in biology and medicine. Among noble metal particles, gold nanoparticles have attracted intensive interest because they are easily prepared, have low toxicity and can be readily attached to molecules of biological interest [10]. An influence of the temperature on the SPR of metal nanoparticles is crucial for pure and applied science [11, 12]. The temperature dependence of the SPR resonance is important because of the recent applications of noble metal nanoparticles in thermally assisted magnetic recording [13] thermal cancer treatment [14-17] catalysis and nanostructure growth [18] and computer chips [19]. Tunability of SPR of noble metal nanoparticles have been achieved by incorporating them into oxide based matrix. Uniformly distributed in various oxide based matrices like SiO_2, ZnO, MgO, TiO_2, etc. are promising candidate for optical applications. Of all oxide based matrices, alumina oxide (Al_2O_3) is one of the most attractive material particularly because of its thermal and chemical stability, excellent dielectric properties, good adhesion to many surfaces and similar band gap (8.8 eV) to SiO_2 [20]. It makes a promising candidate for replacing SiO_2 for gate dielectrics. For these reasons, it is the mostly used host material. Y. Hosoya et al. [21] prepared Au-particle-doped Al_2O_3 films by a sol-gel method and achieved the large nonlinear optical susceptibility and short relaxation time of the film. García-Serrano et al. [22] prepared Au/Al_2O_3 composite thin film by radio-frequency co-sputtering technique and found that the apparent optical absorption band due to the SPR of Au particles appeared and the intensity of the SPR absorption band characteristic of Au nanoparticles increased with the increase of Au particle size. Serna et al. [23] prepared the Cu/Al_2O_3 nanocomposite thin films by alternate pulsed laser deposition from pure metallic Cu and ceramic Al_2O_3 targets. The films showed a nonlinear optical response that is modified by laser irradiation.

A large number of methods have been used to obtain AuNPs embedded in Al_2O_3 films such ion implantation [24-27], sol-gel [21, 28], Laser evaporation and cluster deposition [29-32], and RF magnetron sputtering [22, 33-35].The flexibility and easy fabrication of diverse composite films are the advantages of sputtering method.

In this work, Au/Al_2O_3 nanocomposite films were synthesized on glass substrate at room temperature by RF-magnetron sputtering technique. The as-deposited and heat-treated films were characterized by X-ray diffraction and optical absorption spectroscopy. Evolution of structural and optical properties of gold nanoparticles in alumina matrix as a function of temperature has been studied.

2. Experimental Methods

Au/Al_2O_3 composite thin films were prepared by RF magnetron sputtering technique using an Alcatel SCM 650 apparatus. The target is constituted by two materials: pure metal Au chips (99.99%) on top of alumina disc of purity 99.99%. The gold to alumina surface ratio is fixed at 1.3%. The chamber was evacuated to a pressure better than 10^{-6} mbar, before the argon gas for the sputtering was introduced. The deposition was accomplished on clean glass substrates at room temperature at a fixed argon pressure of $5x10^{-3}$ mbar. The substrate to target distance, deposition time and applied power were fixed at 60 mm, 4h30min and 50w respectively. The prepared samples were annealed for 1hour at different temperatures.

For analysis of the samples, the structural characterization was carried out using a Siemens D5000 diffractometer, employing CuK_α radiation in the $\theta/2\theta$ configuration. The optical transmission spectra were registered by a Shimadzu UV 3101 PC spectrophotometer in the wavelength range of 300 - 2000 nm.

3. Results and Discussion

3.1 Structural Analysis

Fig. 1 shows the XRD patterns of the Au/Al_2O_3 composite films before and after annealing. It can be seen that the spectra of all the samples had a shoulder around $2\theta = 40°$ and a broad peak at around 64°. The crystalline phases of the Au/Al_2O_3 composite film were determined from a deconvolution procedure of the XRD spectrum with commercial software (program) available on our computer. Note that the purpose of the deconvolution is to fit the measured XRD spectrum in well-defined peaks to which a physical meaning can be attributed. For more details see the

*Corresponding Author
Email Address: ali_chouiyakh@hotmail.com (Ali Chouiyakh)

works [35-37]. After thermal treatment the peak intensities slightly increases evidencing some improvement in film crystallinity. Fig. 2 shows the experimental diffractogram and their curve fitting of the Au/Al_2O_3 composite sample deposited at room temperature. Therefore, the XRD spectra of the composite film have to be deconvoluted with four peaks as illustrated in Fig. 2. The peak centered on 2θ = 26° corresponds to the amorphous alumina. For comparison, X-ray diffractogram of gold thin film with a cubic structure presented as a reference is also reported in Fig. 1 The peak positions are in agreement with the well-known data: IJPDS - 04 - 0784 characteristic of a gold crystal in a cubic phase, indicating that gold particles in different composite films should adopt an fcc-like structure. The peaks are considerably broadened; the extent of broadening is described by full width at half maximum intensity of the peak (FWHM). This broadening of the diffraction peak is related to the size nanoparticle D via the Scherrer's formula: $D = 0.9\lambda/(FWHM)\cos(\theta_B)$, where λ is the X-ray wavelength and θ_B is the Bragg angle of the peak.

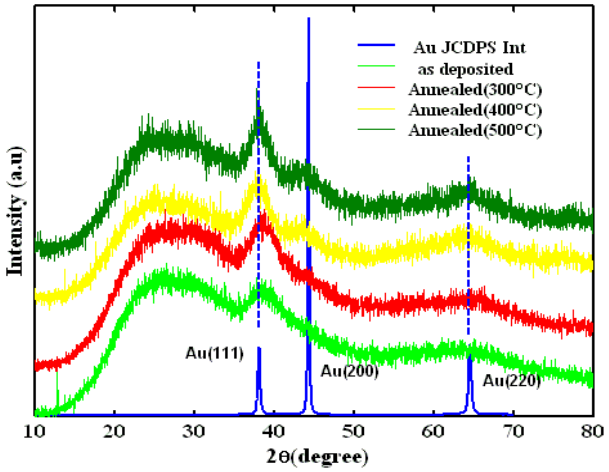

Fig. 1 X-ray diffractograms of Au/Al_2O_3 nanocomposite thin films as-grown, heated at 300 °C, 400 °C, 500 °C and JCPDS of gold thin films

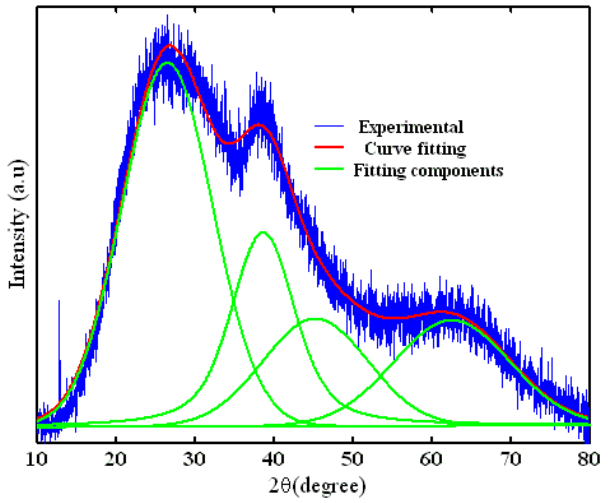

Fig. 2 Experimental diffractogram of the sample deposited at room temperature and their curve fitting where different pseudo-Voigt functions were taken into account

Table 1 Results of the curve fitting of the experimental diffractograms calculated from Au (111) reflections of the as-grown and annealed samples

Temperature (°C)	FWHM (degree)	2θ (degree)	Lattice parameter (Å)	Size(Å)
25	10 .01	38.66	4.034	8.42
300	8.97	38.48	4.051	9.38
400	7.00	38.29	4.070	12.02
500	5.75	38.15	4.085	14.60

Table 1 summarizes the fitting parameters determined from the Au (111) orientation plane for all the samples. This samples indicates that Au NPs size shows an appreciable increase after heat treatment above 300 °C. Then, by varying the annealing temperature, we can control the size of Au nanoparticles. The size varied from 0.84 to 1.46 nm and the lattice constant parameter increased when heat temperature varies from 25 to 500 °C. So, lattice contraction depends implicitly on the particle size.

The concept of surface stress in solids, introduced by Gibbs [38] implies the occurrence of a hydrostatic compression induced by surface/interface stress leading to a change of the lattice parameter, Δa, as compared to the lattice parameter of the undistorted coarse-grained counterpart, a_0, given by Mays et al [39]:

$$\Delta a = -\frac{4}{3D} k f a_0 \qquad (1)$$

Where f is the surface/interface tension, D is the spherical grain diameter and k is the bulk modulus. With decreasing grain size, the effect of surface/interface stress will become significant and a lattice contraction is observed. Therefore, a measure of the lattice variation parameter Δa allows us to determine the surface stress f. The graphical representation of the lattice spacing versus the reciprocal diameter of gold nanoparticle is shown in Fig. 3. So, from the slope of the linear regression, the interface stress is evaluated according to the Eq. (1) with the value for the compressibility of bulk gold, K = 5.848 x 10^{-12} Pa^{-1} [40]. The value of f = 3.11 N/m has been obtained for gold clusters embedded in alumina matrix. A comparison to published experimental f coefficients shows that the determined surface stress value is lower than f = 3.83 N/m, determined by Solliard et al [41] and in good agreement with, f = 3.2N/m, determined in the work [36].

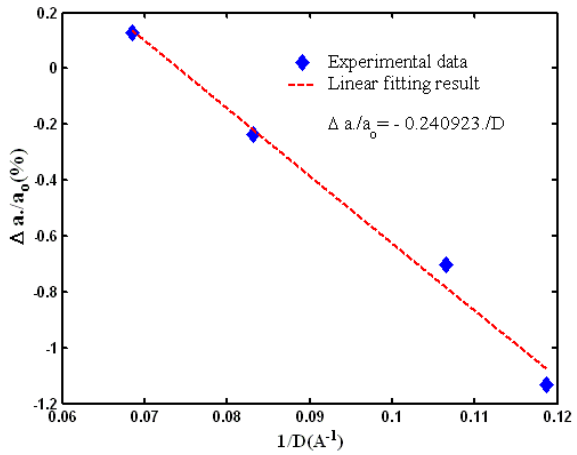

Fig. 3 variation of the relative lattice parameter $\Delta a/a_0$ as a function of the reciprocal diameter of Au nanoparticles embedded in alumina matrix

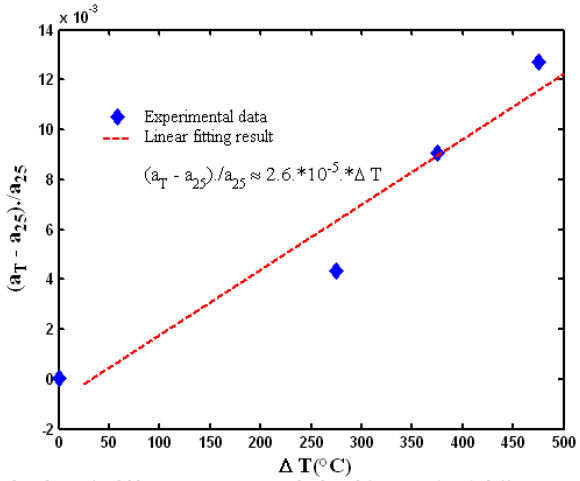

Fig. 4 The plots of gold lattice parameter, calculated from Au (111) diffraction versus temperature

An important aspect in this work is the thermal behavior that the metallic nanoparticle presents during heating. The lattice thermal expansion (α_{gold}) whose value depends on the temperature can be calculated by the following relationship:

$$\frac{a_T - a_{25}}{a_{25}} = \alpha_{gold}\,\Delta T \qquad (2)$$

Where T is the annealing temperature and $\Delta T = T - 25$ °C.

It can be seen from Fig. 4 that the evolution of lattice constant shows roughly linear relation with increasing temperature. The lattice thermal expansion coefficient obtained is 2.6 x 10^{-5}/°C, which is a factor of 2 times larger than that of the bulk Au(1.4 x 10^{-5}/°C).

3.2 Optical Characterization

The optical absorption spectra for the as-deposited and for the various heat-treated nanocomposite films are shown in Fig. 5. The spectra revealed an absorption in the short wavelength region of <450 nm, which is due to 5d to 6sp inter-band transition [22] and exhibit a broad absorption band at around 500 nm, which was assigned to the SPR of Au particles. The intensity of the SPR absorption band increased progressively with the increase of the annealing temperature of the films. This effect is attributed to the increment in the particle size caused as mentioned above by the increase of the annealing temperature of the samples, since the SPR absorption of small metal particles is originated from the collective motion of the conduction electrons interacted with external electromagnetic field of the incident radiation. The measured optical absorption curves were modeled based on Mie theory taking into account the mean free path of gold bulk conduction electrons. Using for gold nanoparticles the same values of plasma frequency, Fermi velocity, damping constant and the scattering parameter, w_P,v_F,Γ, A, respectively cited in the work [35-37]. Theoretical absorption spectra were also calculated by a combination of the same Eqs. (1) and (2) used in this work. The dielectric constant values of the bulk were taken from [42].

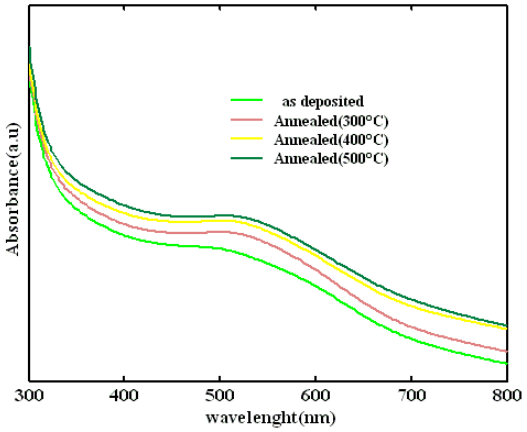

Fig. 5 Optical absorption spectra of Au/Al_2O_3 thin films as-deposited and at different annealing temperatures

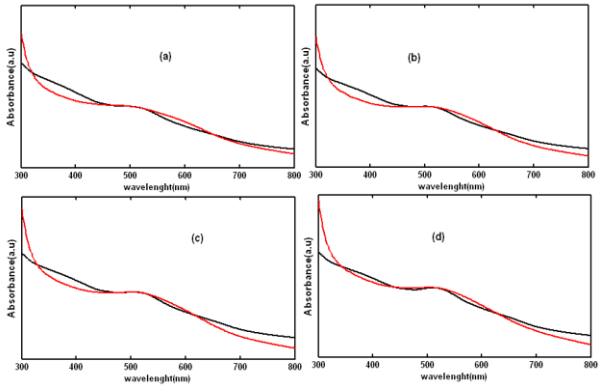

Fig. 6 Experimental and Mie simulated optical absorption spectra for the films as deposited (a) annealed at (b) 300 °C, (c) 400 °C and (d) 500 °C

Figs. 6(a-d) show the simulation and the experimental absorption spectra. The simulation results are summarized in Table 2. The plasmon peak positions just vary from 495 nm to 511 nm and the size increases slightly from 2.0 nm to 2.5 nm when heating temperature increases from 25 °C to 500 °C. The variation of SPR peak position (λ_{max}) with the annealing temperature is reported in Fig. 7. The solid line is a linear fit to the experimental data corresponding to the absorption maxima as determined from the calculated spectra in Fig. 6. An equation is derived in order to predict the maximum plasmon wavelength λ_{max} at different temperatures.

$$\lambda_{max} = 3.25.10^{-2}\Delta T+495 \quad (3)$$

The value of 495 nm represents the SPR at room temperature. The Au nanparticle sizes estimated from optical absorption spectra are larger than those measured from XRD. It is probably due to that the Scherrer's equation is based on size limited bulk structure and relating particle size to the peak width, cannot be used with great accuracy for very small clusters [43]. Formation of gold nanoparticles embedded in silica films using RF-magnetron sputtering technique with subsequent thermal treatment in the same range of temperature have been reported in the work [36]. These authors found that after heat treatment the size and the lattice parameter increases, while the SPR red shift from 500 to 505 nm. In another work [35] the authors investigated the surface plasmon of gold clusters embedded in alumina matrix found that the peak position of the SPR exhibits a linear dependence with lattice parameter.

Table 2 Plasmon peak position, size and dielectric functions of the surrounding medium of the sample as-deposited and heating at different temperatures

Annealing Temperature (°C)	SPR (nm)	Size (nm)	ε_m
25	495	2	3
300	503	2.2	3
400	506	2.3	3
500	511	2.5	3

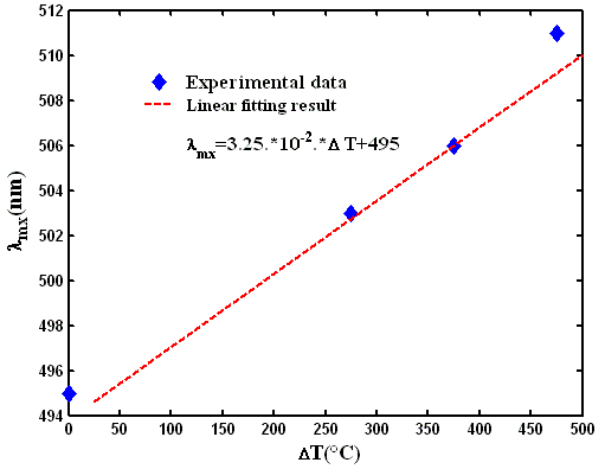

Fig. 7. Variation of surface plasmon resonance peak position (λ_{max}) with annealing temperatures

The heat treatment annealing process is the most important and effective method to control the nanoparticle size. Independently of the production technique, several authors report different post-annealing effects. Hence, the temperature effects on the SPR absorption band of metal NPs were studied by Kreibig [11, 44, 45] and Doremus [46, 47], and the origin of temperature effects upon the SPR was analyzed by Mulvaney [48]. Recently, the influence of temperature on SPR in Ag, Au and Cu NPs at high temperatures was reported in the works [49-52] and the results of a similar study of Au-based plasmonic nanostructures at low temperatures were reported in work [53], where appreciable red-shift and broadening of the SPR with increasing temperature were observed.

About the peak position of the SPR, except for the well-known blue shift effect of the SPR peak as a function of decreasing particles radius a redshift induced by the strong matrix effect has also be found by Smithard [54]. Kreibig and Vollmer [11] pointed out the numerous experiments performed on Ag_n clusters had proved the sensitivity of the size evolution of the Mie frequency on the surrounding matrix. Palpant and coworkers [55] investigated the surface plasmon energy of silver clusters in the framework of the time-dependent local density approximation (TDLDA), and found that the various observed size trends may be conclusively explained by simple dielectric effect. They also proved theoretically that the size effects are very sensitive to the matrix, the porosity at the interface.

4. Conclusion

In this work, thin films of Au-alumina nano composite deposited by co-sputtering technique have been investigated. XRD studies confirmed the presence of Au nanoparticles in amorphous alumina matrix. The lattice parameter exhibits a linear dependence with annealing temperature and thermal expansion coefficient of gold is deduced. Regular red shift in SPR with tunability from 495 to 511 nm is achieved after post heat treatment. The observed redshift of SPR varies linearly with annealing temperature is explained on the basis of increased particle size of Au nanoparticles and are in agreement with modified Mie theory.

Acknowledgment

We are grateful to Professor M.J.M. Gomes from the Centre of Physics, University of Minho, Portugal, for the experimental support.

References

[1] J. Toudert, L. Simonot, S. Camelio, D. Babonneau, Advanced optical effective medium modeling for a single layer of polydisperse ellipsoidal nanoparticles embedded in a homogeneous dielectric medium: Surface plasmon resonances, Phys. Rev. B 86 (2012) 45415-45430.

[2] E. Petryayeva, U.J. Krull, Localized surface plasmon resonance: Nanostructures, bioassays and biosensing-A review, Anal. Chim. Act. 706 (2011) 8-24.

[3] E. Hutter, J.H. Fendler, Exploitation of localized surface plasmon resonance, Adv. Mater. 16 (2004) 1685-1706.

[4] K.A. Willets, R.P. Van Duyne, Localized surface plasmon resonance spectroscopy and sensing, Annu. Rev. Phys. Chem. 58 (2007) 267-297.

[5] K. Lance Kelly, E. Coronado, L.L. Zhao, G.C. Schatz, The optical properties of metal nanoparticles: the influence of size, shape and dielectric environment, J. Phys. Chem. B 107 (2003) 668-677.

[6] S. Palomba, L. Novotny, R.E. Palmer, Blue-shifted plasmon resonance of individual size-selected gold nanoparticles, Opt. Commun. 281 (2008) 480-483.

[7] D.K. Avasthi, Y.K. Mishra, D. Kabiraj, N.P .Lalla, J.C. Pivin, Synthesis of metal-polymer nanocomposite for optical applications, Nanotech. 18 (2007) 125604-125607.

[8] M.G. Muro, Z. Konstantinovic, M. Varela, X. Batlle, A. Labarta, Metallic nanoparticles embedded in a dielectric matrix: growth mechanisms and percolation, J. Nanomater. 2008 (2008) 59-63.

[9] B. Balamurugan, T. Maruyama, Evidence of an enhanced inter-band absorption in Au nanoparticles: size-dependent electronic structure and optical properties, Appl. Phys. Lett. 87 (2005) 143105-143105.

[10] Y. Chen, J.A. Preece, R.E. Palmer, Processing and characterization of gold nanoparticles for use in plasmon probe spectroscopy and microscopy of biosystems, Ann. N.Y. Acad. Sci. 1130 (2008) 201-206.

[11] U. Kreibig, M. Vollmer, Optical properties of metal clusters, Springer, Berlin, 1995.

[12] O.A. Yeshchenko, I.S. Bondarchuk, V.S. Gurin, I.M. Dmitruk, A.V. Kotko, Temperature dependence of the surface plasmon resonance in gold nanoparticles, Surf. Sci. 608 (2013) 275-281.

[13] W.A. Challener, C. Peng, A.V. Itagi, D. Karns, W. Peng, Y. Peng, et al, Heat-assisted magnetic recording by a near-field transducer with efficient optical energy transfer, Nat. Photon 3 (2009) 220-224.

[14] D.P.O. Neal, L.R. Hirsch, N.J. Halas, J.D. Payne, J.L. West, Photo-thermal tumor ablation in mice using near infrared-absorbing nanoparticles, Cancer Lett. 209 (2004) 171-176.

[15] L.R. Hirsch, R.J. Stafford, J.A. Bankson, S.R. Sershen, B. Rivera, R.E. Price, et al, Nanoshell-mediated near-infrared thermal therapy of tumors under magnetic resonance guidance, Proc. Natl. Acad. Sci. USA 100 (2003) 13549-13554.

[16] A. Lowery, A. Gobin, E. Day, N. Halas, J. West, Immuno nanoshell laser-assisted therapy targets and ablates tumor cells, Breast Cancer Res. Treat. 100 (2006) 289.

[17] A. Lowery, A. Gobin, E. Day, N. Halas, J. West, Immuno nanoshells for targeted photothermal ablation of tumor cells, Int. J. Nanomed. 1 (2006) 149-154.

[18] L. Cao, D.N. Barsic, A.R. Guichard, M.L. Brongersma, Plasmon-assisted local temperature control to pattern individual semiconductor nanowires and carbon nanotubes, Nano. Lett. 7 (2007) 3523-3527.

[19] W. Cai, J.S. White, M.L. Brongersma, Compact, high-speed and power-efficient electrooptic plasmonic modulators, Nano. Lett. 9 (2009) 4403-4411.

[20] L. Manchanda, M.D. Morris, M.L. Green, R.B. van Dover, F. Klemens, T.W. Sorsch, et al, Multi-component high-K gate dielectrics for the silicon industry, Microelectron. Eng. 59 (2001) 351-359.

[21] Y. Hosoya, T. Suga, T. Yanagawa, Y. Kurokawa, Linear and nonlinear optical properties of sol-gel-derived Au nanometer-particle-doped alumina, J. Appl. Phys. 81 (1997) 1475-1480.

[22] J. Garcia-Serrano, U. Pal, Synthesis and characterization of Au nanoparticles in Al_2O_3 matrix, Int. J. Hydrogen Energy 82 (2003) 637-640.

[23] R. Serna, J.M. Ballesteros, J. Solis, C.N. Afonso, D.H. Osborne, R.F. Haglund, et al, Laser-induced modification of the nonlinear optical response of laser-deposited Cu: Al_2O_3 nanocomposite films, Thin Sol. Films 318 (1998) 96-99.

[24] D. Dhara, B. Sundaravel, T.R. Ravindran, K.G.M. Nair, C. David. B.K. Panigrahi, et al, Spill out effect in gold nanoclusters embedded in c-Al_2O_3 (0001) matrix, Chem. Phys. Lett. 399 (2004) 354-358.

[25] M. Ohkubo, N. Susuki, Morphology of small gold crystals formed inside sapphire by ion implantation, Philos. Mag. Lett. 57 (1988) 261-265.

[26] D.O. Henderson, R. Mu, Y.S. Tung, M.A. George, A. Burger, S.H. Morgan, et al, Atomic force microscopy of Au implanted in sapphire, J. Vac. Sci. Technol. B 13 (1995) 1198-1202.

[27] C. Margues, E. Alves, R.C. da Silver, M.R. Silva, A.L. Stepanov, Optical changes induced by high fluence implantation of Au ions on sapphire, Nucl. Instrum. Meth. Phys. Res. B 208 (2004) 139-144.

[28] S. Muto, T. Kubo, Y. Kurokawa, K. Suzuki, Third-order nonlinear optical properties of Disperse Red 1 and Au nanometer-size particle-doped alumina films prepared by the sol-gel method, Thin Sol. Films 322 (1998) 233-237.

[29] J. Lermé, B. Palpant, B. Prével, E. Cottancin, M. Pellarin, M. Treilleux, et al, Optical properties of gold metal clusters: A time-dependent local-density-approximation investigation, Eur. Phys. J. 4 (1998) 95-108.

[30] B. Palpant, B. Prével, J. Lermé, E. Cottancin, M. Pellarin, M. Treilleux, et al, Optical properties of gold clusters in the size range 2-4 nm, Phys. Rev. B 57 (1998) 1963-1970.

[31] E. Cottancin, J. Lermé, M. Gaudry, M. Pellarin, J.L. Vialle, M. Broyer, et al, Size effects in the optical properties of Au n Ag n embedded clusters, Phys. Rev. B 62 (2000) 5179-5185.

[32] M. Gaudry, J. Lermé, E. Cottancin, M. Pellarin, J.L. Vialle, M. Broyer, et al, Optical properties of (Au_xAg_{1-x})(n)clusters embedded in alumina: Evolution with size and stoichiometry, Phys. Rev. B 6408 (2001) 5407-5413.

[33] H.B. Liao, R.F. Xiao, J.S, Fu, G.K.L. Wong, Large third-order nonlinear optical susceptibility of Au-Al_2O_3 composite films near the resonant frequency, Appl. Phys. B 65 (1997) 673-676.

[34] J. Wang, W.M. Lau, Q. Li, Effects of particle size and spacing on the optical properties of gold nanocrystals in alumina, J. Appl. Phys. 97 (2005) 114303-114310.

[35] A. Belahmar, A. Chouiyakh, Influence of the fabrication conditions on the formation and properties of gold nanoparticles in alumina matrix produced by co-sputtering, Int. J. Nano. Mater. Sci. 3 (2014) 16-29.

[36] A. Belahmar, A. Chouiyakh, Effect of post-annealing on structural and optical properties of gold nanoparticles embedded in silica films grown by RF-sputtering, Adv. Phys. Theory Appl. 15 (2013) 38-46.

[37] A. Belahmar, A. Chouiyakh, Investigation of surface plasmon resonance and optical band gap energy in gold/silica composite films prepared by rf-sputtering, Int. J. Nanosci. Tech. 2(2) (2016) 81-84.

[38] J.W. Gibbs, Collected works, Longmans green and company, New York, 1928.

[39] C.W. Mays, J.S. Vermaak, D. Kuhlmann-Wilsdorf, On surface stress and surface tension: II: Determination of the surface stress of gold, Surf. Sci. 12 (1968) 134-140.

[40] Q. Jiang, L.H. Liang, D.S. Zhao, Lattice contraction and surface stress of fcc Nanocrystals, J. Phys. Chem. B 105 (2001) 6275-6277.

[41] C. Solliard, Ph. Buffat, Variation de la maille cristalline de petits cristaux d'or par effet de taille, J. Phys. Colloq. 38 (1977) 167-170.

[42] E.D. Palik, Handbook of optical Constants of Solids, Academic Press, New York, 1991.

[43] J.B. Cohen, X-ray diffraction studies of catalysts, Ultramicroscopy 34 (1990) 41-46.

[44] U. Kreibig, Anomalous frequency and temperature dependence of the optical absorption of small gold particles, J. Phys. Colloq. 38 (1977) 97-103.

[45] U. Kreibig, Electronic properties of small silver particles: the optical constants and their temperature dependence, J. Phys. F. Metal Phys. 4 (1974) 999-1014.

[46] R.H. Doremus, Optical properties of small gold particles, J. Chem. Phys. 40 (1964) 2389-2396.

[47] R.H. Doremus, Optical properties of small silver particles, J. Chem. Phys. 42 (1965) 414-417.

[48] P. Mulvaney, Nanoscale materials in chemistry, Wiley, New York, 2001, pp.121-167.

[49] O.A. Yeshchenko, I.M. Dmitruk, A.A. Alexeenko, A.V. Kotko, J. Verdal, A.O. Pinchuk, Size and temperature effects on the surface plasmon resonance in silver nanoparticles, Plasmonics 7 (2012) 685-694.

[50] O.A. Yeshchenko, I.S. Bondarchuk, A.A. Alexeenko, A.V. Kotko, Temperature dependence of the surface plasmon resonance in silver nanoparticles, Funct. Mater. 20 (2013) 357-365.

[51] O.A. Yeshchenko, I.S. Bondarchuk, V.S. Gurin, I.M. Dmitruk, A.V. Kotko, Temperature dependence of the surface plasmon resonance in gold nanoparticles, Surf. Sci. 608 (2013) 275-281.

[52] O.A. Yeshchenko, Temperature effects on the surface plasmon resonance in copper nanoparticles, Ukr. J. Phys. 58 (2013) 249-259.

[53] J.S.G. Bouillard, W. Dickson, D.P. O'Connor, G.A. Wurtz, A.V. Zayats, Low-temperature plasmonics of metallic nanostructures, Nano. Lett. 12 (2012) 1561-1565.

[54] M.A. Smithard, Size effect on the Mie optical absorption of small sodium particles in sodium azide NaN_3, Solid State Commun. 14 (1974) 407-410.

[55] J. Lerme, B. Palpant, B. Prevel, M. Pellarin, M. Treilleux, J.L. Vialle, et al, Quenching of the size effects in free and matrix-embedded silver clusters, Phys. Rev. Lett. 80 (1998) 5105-5108.